The Aeronautical Journal (2026), **130**, pp. 657–679
doi:10.1017/aer.2025.10098

ROYAL AERONAUTICAL SOCIETY

RESEARCH ARTICLE

Tab orientation effect on jet mixing

E. Rathakrishnan

Department of Aerospace Engineering, Indian Institute of Technology Kanpur, Kanpur, India
Corresponding author: Email: erath@iitk.ac.in

Received: 28 January 2025; **Revised:** 20 October 2025; **Accepted:** 21 October 2025

Keywords: compressible; core; jet; Mach number; mixing

Abstract

The effect of tab orientation on the mixing characteristics of a Mach 1.6 circular jet issuing from a convergent-divergent (C-D) nozzle is studied experimentally. The tabs used in this study are triangular tabs with sharp and truncated vertices positioned upright and in inverse orientations, along diametrically opposite locations at the nozzle exit. Mixing characteristics of the jet operated at nozzle pressure ratios (NPRs) 3 to 6, in step 1, were studied. For inverse triangular and inverse truncated triangular tabs, a maximum core length reduction of about 87% is achieved at NPR 3. The corresponding core length reductions caused by the upright triangular and truncated triangular, and rectangular tabs are 71, 81 and 84%, respectively. It is found that the jet mixing is strongly influenced by the combined effect of tab geometry, tip effectand the pressure gradient at the nozzle exit. The pressure distribution in the directions along and perpendicular to the tab, at different axial locations, was used to discern the evolution and spread of the jet. The pressure profiles for all tab geometries show that the jet spread perpendicular to the tab is more than that along the tab at all the NPRs studied. The shadowgraph images of the jets show that the waves present in the controlled jet are weaker than those in the uncontrolled jet.

Nomenclature

CPD	centreline pressure decay
D	nozzle exit diameter
NPR	nozzle pressure ratio
P_a	atmospheric pressure
P_b	nozzle backpressure
P_e	pressure at nozzle exit
P_0	settling chamber stagnation pressure
P_t	pitot pressure
T_a	atmospheric temperature
X	distance along the x-axis from the nozzle exit plane
Y	distance along the y-axis away from the nozzle centreline
Z	distance along the z-axis away from the nozzle centreline

1.0 Introduction

Jet is a free shear flow driven by the momentum of fluid emanating from a nozzle or orifice and exhibits a characteristic that the ratio of width-to-axial distance remains constant [1]. The jet can also be defined as a fluid flow on either side of tangential separation surfaces. Jets are generally turbulent and characterised by the presence of both large-scale coherent structures and small-scale vortical structures. The large-scale coherent structures are known to be predominantly involved in the entrainment of ambient fluid into the jet stream whereas small-scale vortices promote better mixing. The continuous entrainment of ambient fluid progressively increases the mass flow rate along the jet downstream. Hence, to

© The Author(s), 2025. Published by Cambridge University Press on behalf of Royal Aeronautical Society.

https://doi.org/10.1017/aer.2025.10098 Published online by Cambridge University Press

comply with Newton's second law jet centreline velocity continuously reduces with downstream distance. The orifice/nozzle exit geometry plays a vital role in the evolution of the jet. By employing a non-circular exit geometric shape, the entrainment and mixing of the jet with the entrained fluid mass can be enhanced significantly [2–5]. In many technological applications of jets, such as fuel-air mixing in the combustion chamber, reducing infrared signature and noise level of jet, rapid mixing of jet with the surrounding fluid is required. Non-circular jets through their complex flow mechanism are beneficial from this point of view. Elliptic jets with non-uniform curvature at the orifice/nozzle exit have many advantages over circular jets. The entrainment, mixing and spread rate of elliptic jets are much higher than the circular jets. Several studies have been done on elliptic jets to prove their superiority over circular ones. The superior mixing capability of elliptic jets compared to their circular counterparts is due to the generation of azimuthal vortices of continuously varying size, generated at the nozzle exit [6].

The different portions of the jet structure can be distinguished as potential core region, transition zone and fully developed region. The core region consists of constant axial velocity equal to the jet (nozzle) exit velocity, surrounded by a rapidly growing and predominantly shear, dominated annulus of mixing layer or shear layer with intense turbulence. The transition region is the region where the centreline velocity begins to decay. This characteristics zone extends from about $5D$ to $10D$ downstream, over which the turbulence changes from its annular to a somewhat pseudo-cylindrical distribution. As a result, the velocity difference between the ambient fluid and the high-speed core region of the jet decreases and attenuates the shear that supports the vertical rings in the jet, and thus the velocity profiles become smoother with jet propagation. The transition region is characterised by a growth of three-dimensional flow due to wave instability of the cores of the vortex rings. The merging of these distorted vortices produces large eddies that can remain coherent around the potential core region of the jet. A fully developed region is beyond the transition region where the jet becomes similar in appearance to a flow of fluid from a source of infinitely small thickness (in an axially symmetric case the source is a point, and in a plane parallel case it is a straight line perpendicular to the plane of the flow of the jet). Jets with Mach numbers between 1 and 4 belong to the regime of supersonic jets. The variation in backpressure concerning stagnation chamber pressure gives rise to different expansion levels. These variations result in the shock cell structures in the jet core. The core region in this case is identified as the extent to which supersonic flow prevails along the jet centreline. This axial extent from the nozzle exit, to which supersonic flow prevails or the axial distance after which the characteristic decay begins is referred to as jet core length. This length can be taken as an authentic measure of near-field mixing of supersonic-free jets [1]. A jet is said to be correctly expanded when the nozzle exit pressure is equal to the ambient pressure. The phenomenon of overexpansion takes place for supersonic jets when nozzle exit pressure is lesser than the backpressure and such jets are referred to as overexpanded jets. A jet is said to be underexpanded when the nozzle exit pressure (P_e) is higher than the backpressure (P_b).

The diverse nature of the applicability of jets demands that they be made suitable for a specific application by controlling them. Here, control may be defined as the ability to modify the jet flow mixing characteristics to achieve engineering efficiency, technological ease, economy, adherence to standards and so on.

All types of jet controls can be broadly classified into active and passive controls. Among the two main types of control, passive controls are mostly desired not only because no external power source is required, but since in some cases the engineer is left with no other options. Passive control methods use geometrical modifications that alter the flow structure. Passive control techniques range from alterations in the exit shape of the nozzle to the implementation of tooth-like tabs and vortex generators in the jet.

The present investigation aims to understand the role of jet control in the form of rectangular and triangular shapes with sharp and truncated vertex, placed upright and inverse orientations (triangular, inverse triangular, truncated triangular and inverse truncated triangular tabs). The mixing promoting

https://doi.org/10.1017/aer.2025.10098 Published online by Cambridge University Press

small-scale vortices generated by the tab alters the mixing of the jet mass and the mass of the surrounding atmosphere entrained into the jet by the mass entraining large-scale vortices formed at the periphery of the jet.

A tab is essentially a small solid strip kept normal to the flow, usually at the nozzle exit, which generates a pair of counter-rotating transverse vortices (with the axis of rotation along the tab) that become streamwise soon after shedding, and can affect the jet flow development significantly. Bradbury and Khadem [7] were the first to conduct a study on the jet flow field under the influence of tabs. They investigated the influence of rectangular tabs in a subsonic jet. The authors contemplated two possible mechanisms by which gross distortion on this scale could occur, namely (i) by the stirring action of trailing vortex motions shed from the tabs and (ii) by the simple deflection of the flow over the tabs such as might occur in a potential flow jet with circumferential variations in flow angle.

Ahuja and Brown [8] conducted an experimental study on jet mixing enhancement of heated and unheated, subsonic and underexpanded supersonic model jets by tabs located at the nozzle lip. Relative performance of two, three and four tabs were evaluated. They concluded that the potential core length reduction, marked by the decay of the centreline fully expanded Mach number, showed that the use of tabs led to a considerable enhancement in mixing.

The results showed that the tabs suppressed the axisymmetric large-scale structures in the jets. To explain the increased mixing despite the suppression of this large-scale structure, the authors hypothesised the following possible mechanisms (i) mutual interaction of a train of other large-scale motions present in the interaction could be quasilinear of catastrophic in nature, (ii) hydrodynamic excitation by the vortices shed by the tab [9, 10], (iii) additional entrainment by the enlarged area of the jet perimeter because of the presence of a wedge-like incision in the jet boundary that starts at the tab and continues to enlarge downstream, (iv) by the very fact that use of tabs in supersonic flow, the additional shock waves are generated that slow the flow considerably.

Samimy et al. [11, 12] studied the effect of small tabs on the characteristics of an axisymmetric jet over a Mach number range of 0.3–1.81. They found that the tabs distort the jet cross-section and increase the jet significantly.

Reeder and Zaman [13] found that the flow field distortion produced by the tabs changed drastically if their location was highly varied relative to the nozzle exit. It was observed that a tab located slightly upstream of the nozzle exit caused an ejection of core fluid at the same azimuthal location, and a tab located downstream with a slight gap from the nozzle exit remained practically ineffective.

Zaman [14] found that the vorticity generation by delta-tab results in the enhancement of jet mixing. Rogers and Parekh [15] used vortex generators in a rectangular jet (aspect ratio 2) to increase the entrainment by 50%. Their jet was subsonic, with an exit Mach number 0.6, and the vortex generators were half delta-wings. They considered various combinations of vortex generators and found that the greatest entrainment benefit came when the vortices oriented to provide a bulk movement of fluid down through the jet.

Bohl and Foss [16] inspected the pressure, velocity and streamwise vorticity fields in the near field of a tabbed free jet. Using static pressure measurements, they confirmed the creation of an upstream pressure hill, which produced two regions of concentrated vorticity into the flow on each side of the tab.

Seiner and Grosch [17] studied the jet plume mass flow entrainment rates associated with the introduction of the counter-rotating streamwise vorticity of prism-shaped tabs located at the lip of the nozzle.

Feng and McGuirk [18] investigated underexpanded jet issuing from an axisymmetric nozzle with a major interest in the region immediately after the nozzle exit, where the tab-induced streamwise vortices are formed, and also where the jet cross-section distortion is largest. The Schlieren images clearly showed the significant changes to the core shock cell system that were caused by the induction of tabs. The potential core length was halved, and the centreline velocity decay rate increased.

Behrouzi and McGuirk [19] studied the effect of tab parameters like tab shape, tab number and tab orientation angle on the near field mixing performance using tabs. They found that this performance of

https://doi.org/10.1017/aer.2025.10098 Published online by Cambridge University Press

solid tabs in causing bifurcation of the jet follows the same trend under both subsonic and supersonic conditions, supporting the idea that the dominant features of the streamwise vorticity introduced by the tabs are essentially independent of compressibility.

Thanigaiarasu et al. [20] investigated the effect of tab geometry and its orientation at the nozzle exit, on the evolution of axisymmetric sonic underexpanded and fully expanded jets. The tab used was a hollow semi-circular tube. The near jet flow field was studied for two configurations of the tab, namely, the concave surface facing the flow exiting nozzle (arc-tab facing in) and the convex surface facing the flow (arc tab facing out) for three different protrusions of the tab with blockages area of 3.82, 7.64 and 11.46%, respectively.

Rathakrishnan [21] assessed the effectiveness of passive control in the form of a cross-wire at the nozzle exit on the decay and noise characteristics of supersonic jets at different levels of expansion. The introduction of streamwise vortices by the cross-wire enhanced the mixing of the jet mass with the mass entrained from the surroundings and weakened the shocks in the jet core significantly, resulting in a considerable reduction of shock-associated noise.

Chiranjeevi and Rathakrishnan [22] examined the efficiency of corrugated tabs in promoting the mixing of supersonic axisymmetric jets. Two rectangular tabs of 4.2% blockage, with straight corrugation along the edges, located diametrically opposite at the exit of Mach 1.8 convergent-divergent nozzle were found to be better mixing promoters than identical rectangular tabs without corrugations. As high as 78% reduction in core length was achieved with corrugated tabs for the jet operated at a nozzle pressure ratio of 7, the corresponding reduction with the plain tabs was only 54%. The effectiveness of corrugated tabs was further verified quantitatively by shadowgraph pictures of uncontrolled and controlled jets.

Triangular tabs for supersonic jet mixing enhancement were studied by Arun Kumar and Rathakrishnan [23, 24]. The results demonstrate that the mixing caused by the right-angled triangular tab with a truncated vertex is superior to the identical tab with a sharp vertex and rectangular tab of equivalent blockage. The mixing-promoting efficiency of the tab is found to increase with the increase of the expansion ratio. The study on the effect of truncated triangular tabs for supersonic jet control [24] showed that among the triangular tabs, the one with a truncated vertex is found to be a better mixing promoter than the one with a sharp vertex. The reason for the superiority is envisaged as the tendency of vortices at the tab tip not to interact among themselves and lose energy, as in the case of the sharp vertex.

The study on the effect of tab length on Mach 1.73 jet mixing showed that among the rectangular tabs of three different aspect ratios of 1.0, 1.5 and 2.0 the mixing promoting capability of the tab with an aspect ratio of 1.5 is superior to tabs of aspect ratio 1 and 2 at all nozzle pressure ratio (NPR), except at nozzle pressure ratio 4 which is an overexpanded level [25]. The effect of corrugation on the mixing-promoting performance of a limiting arc-tab has been assessed by studying the decay of a Mach 1.76 jet emerging from a convergent-divergent nozzle, with a limiting arc-tab, with and without corrugation, running along a diameter at the nozzle exit, operated at nozzle pressure ratios of 4.5 and 8. The results show that the mixing promotion caused by the tabs leads to the shortening of the third and fourth shock cells in the jet core [26].

From the literature, it is evident that the mixing promotion caused by a tab is sensitive to the tab geometry and the level of jet expansion. However, these aspects are studied mostly with tabs of specific geometry and specific orientation. Therefore, it will be of value to study the mixing-promoting capability of a tab concerning its orientation, say with the vertex closer to the jet axis and the base closer to the jet axis, in the case of a triangular tab. With this kind of objective the present study aims at addressing the effect of triangular tabs of sharp and truncated vertex positioned upright and inverse orientations, along diametrically opposite locations at the exit of Mach 1.6 convergent-divergent circular nozzle, operated at NPRs 3 to 6, in steps of 1, were studied.

https://doi.org/10.1017/aer.2025.10098 Published online by Cambridge University Press

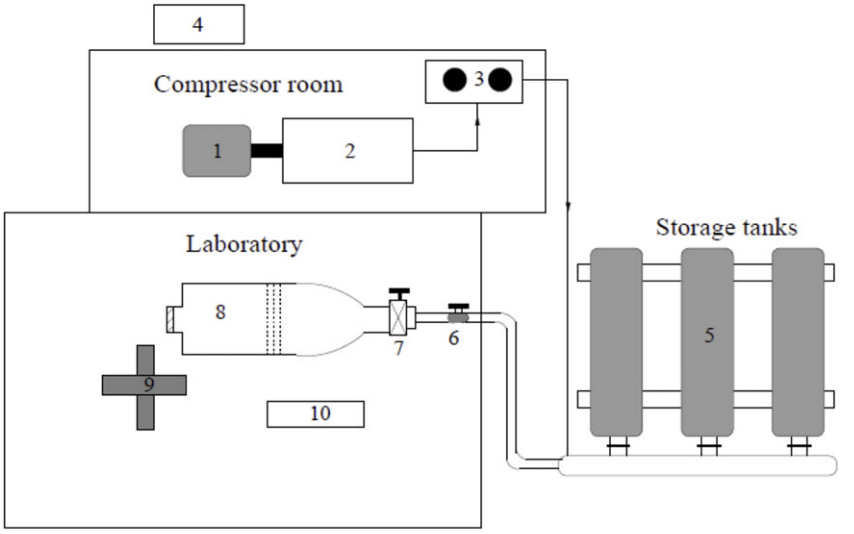


Figure 1. *Laboratory layout of open jet test facility [1].*

2.0 Experimental Setup

The experiments were conducted in the open jet facility at the high-speed aerodynamics laboratory, Indian Institute of Technology Kanpur, India. The test facility consists of a compressed air supply system and an open jet test facility. The layout of the experimental jet facility laboratory is shown in Fig. 1.

The settling chamber is fed air from storage tanks through the air supply system. The compressed air passes through the gate valve, followed by the pressure valve, which is connected to a mixing tube that delivers air to the settling chamber. The settling chamber is connected to the mixing tube through a wide-angle diffuser, which is followed by a few screens or closely meshed grids placed a few centimeters apart to minimise turbulence at the nozzle exit. These screens are inserted in the settling chamber so that air can settle properly. The settling chamber is a constant area circular section with an inside diameter of 300 mm and length of 600 mm. It is provided with ports for measuring the stagnation pressure and temperature. Test models can be fixed at the end of the settling chamber by a slot holder arrangement; a short pipe-like protrusion with an embedded O-ring to prevent leakage. The model used for the study is placed over the O-ring, over which an annular retaining sleeve with internal threads can be screwed tightly. Schematic of the open jet test facility is shown in Fig. 2.

The settling chamber pressure (P_0), can be maintained to attain the desired nozzle pressure ratio (NPR): ratio of stagnation pressure (in settling chamber) to backpressure required (P_0/P_b). The settling chamber temperature was the same as the ambient temperature (T_a), and the backpressure (P_b) was the ambient pressure (P_a) to which the jet was discharged.

The shadowgraph system used had a helium spark arc light source in conjunction with a 150-mm concave mirror of $\lambda/6$ and focal length of 1.6 m, and a screen, illustrated in Fig. 3. The shadowgraph images of the jet on the screen were captured using a SONY 20.4-megapixel DSLR camera.

A pitot tube of 0.4 mm inner diameter and 0.6 mm outer diameter, mounted on a three-dimensional traverse having six degrees of freedom, was used for pressure measurement. Mach 1.6 circular convergent-divergent nozzle of 10-mm exit diameter was used. The ratio of the nozzle exit area to the

https://doi.org/10.1017/aer.2025.10098 Published online by Cambridge University Press

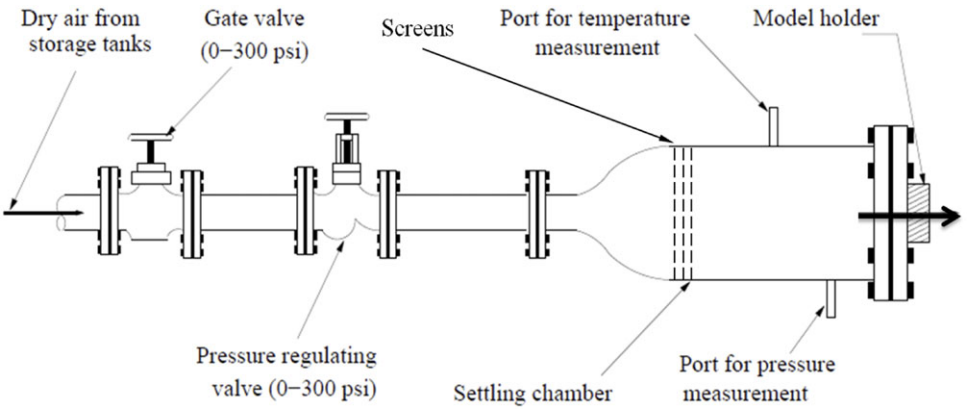


Figure 2. *Schematic diagram of jet test facility.*

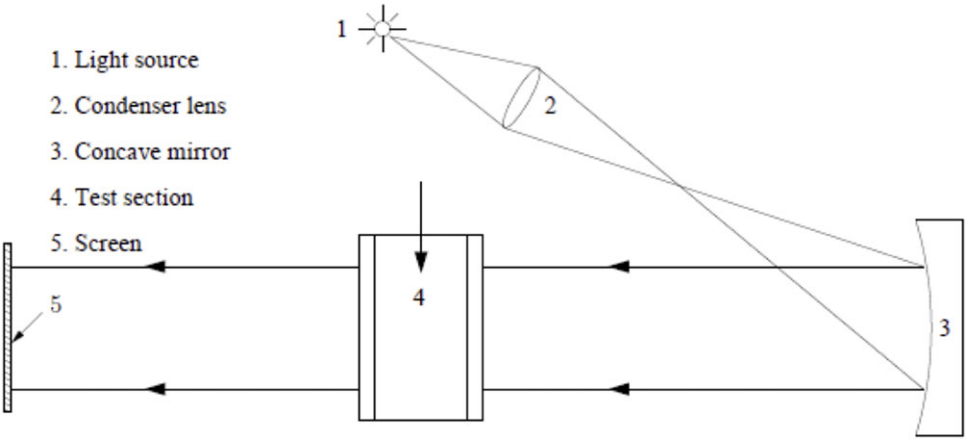


Figure 3. *Shadowgraph system [1].*

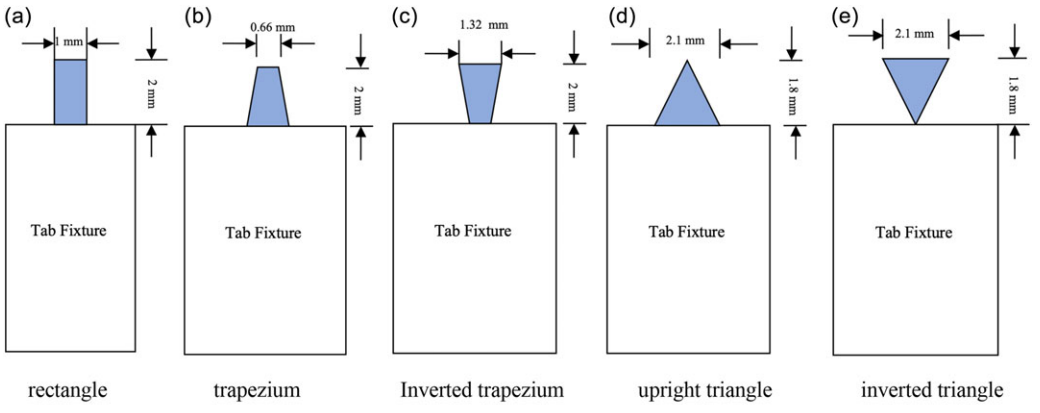
projected area of the probe is kept at more than 64, to ensure that there is no probe blockage effect on the pressure measurement [27]. In all pressure measurements the pitot probe stem was oriented parallel to the y-axis with the probe nose along the jet axis (x-axis). It is to be noted that the pressure measured by the pitot probe in the supersonic regime is not the true total pressure of the flow but it represents the total pressure behind the bow shock formed ahead of the probe nose.

The pitot pressure sensed by the probe was measured using a PSI model-9010, 16-channel pressure transducer interfaced with a Pentium 4 computer loaded with VI-based software for data acquisition. The model-9010 transducer is capable of measuring pressures up to 300 psi. The transducer also has a facility to choose the number of samples to be averaged, using dip-switch settings. The accuracy of the transducer after re-zero calibration is specified to be 0.15% full scale. The application software developed using LabVIEW links the host computer to the pressure scanner via RS 232 communication. The application software performs all the required functions like initialise, reset, re-zero calibration and read pressure. Ambient temperature (T_a) was measured using a thermometer, and ambient pressure (P_a) was measured using a mercury barometer.

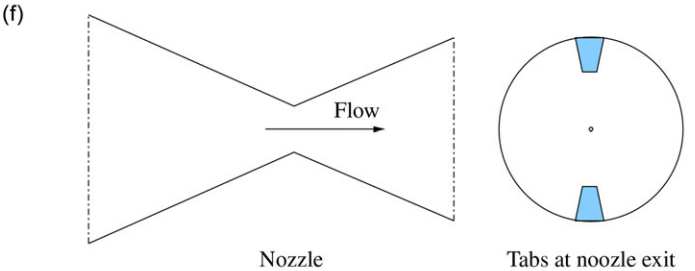
2.1 Experimental model

The experimental model used in the present investigation is a Mach 1.6 convergent-divergent nozzle with a 10 mm exit diameter. The nozzle was fixed at the exit of the settling chamber shown in Fig. 2.

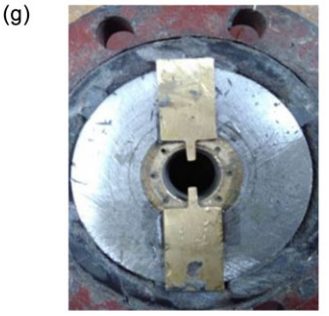
https://doi.org/10.1017/aer.2025.10098 Published online by Cambridge University Press



Schematic sketch of the tabs used.



Schematic sketch of the tabs at the nozzle exit.



A photographic view of the tabs at the nozzle exit.

Figure 4. *(a)–(e) Schematic sketch of the tabs used. (a) rectangle (b) trapezium (c) inverted trapezium (d) upright triangle (e) inverted triangle (f) schematic sketch of the tabs at the nozzle exit (g) photographic view of the tabs at the nozzle exit.*

Schematic diagrams of the tab configurations are given in the Fig 4a–e. A schematic view of the nozzle, along with tabs at the nozzle exit, is shown in Fig. 4f. A photographic view of the tabs at the nozzle exit is shown in Fig. 4g. The nozzle was calibrated after fabrication, because the actual Mach number may differ from the designed Mach number.

Supersonic jets issuing from the convergent-divergent circular nozzle with and without control, at underexpanded and overexpanded conditions in the range of nozzle pressure ratio (NPR) from 3 to 6, were investigated. Mach 1.6 jet is correctly expanded at NPR 4.25. The NPRs 3 and 4 correspond to 29% and 5.9% overexpansion. Whereas, NPR 5 and 6 correspond to underexpansion levels of 18% and

https://doi.org/10.1017/aer.2025.10098 Published online by Cambridge University Press

42%, respectively. As the NPR increases from 3 to 6, the pressure gradient at the nozzle exit changes from adverse to favourable.

The blockage due to the tabs, defined as the ratio of the projected area of the tabs normal to the nozzle axis to the nozzle exit area, was 2.5%.

The centreline pitot pressure distributions of the Mach 1.6 jet, at different levels of expansion, were measured by placing the pitot probe along the jet axis (x-axis), from the exit of the nozzle in the downstream direction. The pitot probe was moved along the jet axis, at intervals of 1 mm up to 200 mm. For correctly expanded, overexpanded and underexpanded conditions, in the supersonic regimes of the jet, the measured stagnation pressure (P_0) corresponds to the stagnation pressure behind the standing bow shock in front of the pitot tube.

The changes introduced in the presence of tabs on the spread characteristics of supersonic jets at different levels were investigated by plotting pressure profiles. This was carefully done by first identifying the extremes along either axis of the jet field and then recording pitot pressure values in between them at intervals of 1 mm.

2.2 Data accuracy

In the supersonic region, there will be some measurement error due to probe interference with shock structure so the measured values must be considered qualitatively good enough for comparative study only. The room temperature was almost constant with a maximum variation of ± 0.5 % during an experimental run. Since the nearest wall downstream to the nozzle exit was around 3.5 m away the wall effects were assumed to be negligible. The stagnation pressure in the settling chamber was maintained at a specified level for a particular run within the uncertainty of ± 1%.

3.0 Results and Discussion

The measured data consists of the pitot pressure variation along the jet axis (x-direction), in the directions perpendicular to the tab (z-direction) and along the tab (y-direction). The measured pressures are presented as such, in the non-dimensional form, because calculating the Mach number from the measured pressure is impossible for the present field because of the complex wave pattern prevailing in the jet field.

3.1 Centreline pressure decay

The centreline pressure decay (CPD) can give an authentic quantification of the core length, characteristic decay rate and far-field decay. Also, the strength of compression and expansion waves present in the core of a supersonic jet, and the length of shock cells in the core can be discerned from the centreline pressure decay. With this aim, the pressure variation along the jet axis was measured with a pitot probe. The measured data is made non-dimensional by dividing the pitot pressure (P_t) with the settling chamber pressure (P_0). The axial distance (x) is made non-dimensional by dividing it by the diameter of the nozzle exit (D). The variation of P_t/P_0 with X/D, for the tested NPRs of 3, 4, 5 and 6, are presented in Figs. 5–8. For the Mach 1.6 jet, the NPR for correct expansion is 4.2. Thus the range of NPRs in the present work covers overexpansion, almost correct expansion and underexpansion. Control of the jet mixing with tabs was studied for the five tab configurations shown in Fig. 3a–e. For every tab configuration experiments were conducted for NPRs 3, 4, 5 and 6.

The CPD of the uncontrolled and controlled jets, for NPR 3, are compared shown in Fig. 5

It is seen that a considerable number of compression and expansion waves are present in the core; the distance from nozzle exit and point at which characteristics decay begins. For Mach 1.6 jet, NPR 3 corresponds to 29% overexpansion ($P_e/P_a = 0.71$). For this case, there should be an oblique shock at the nozzle exit to increase the pressure to come to an equilibrium with the backpressure, which is the

https://doi.org/10.1017/aer.2025.10098 Published online by Cambridge University Press

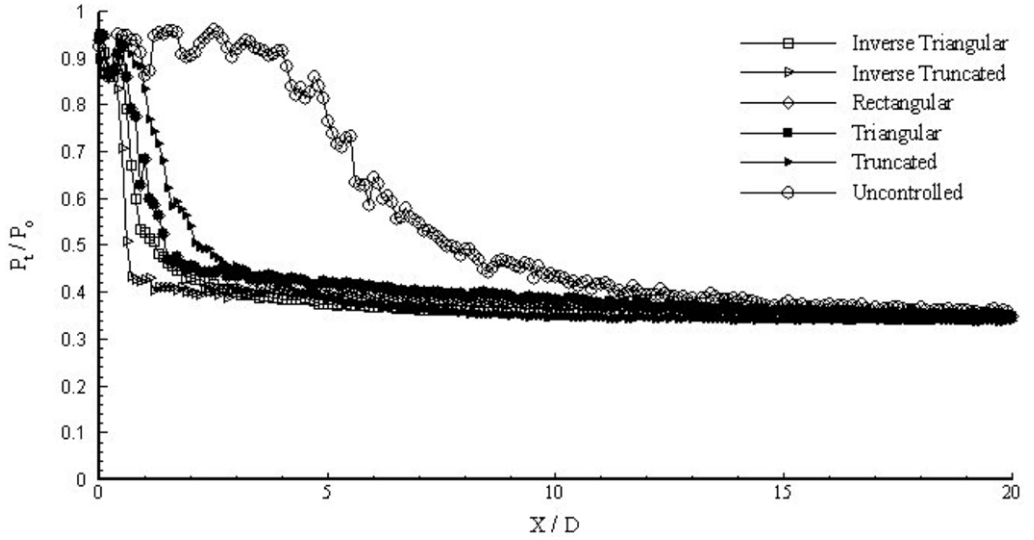


Figure 5. *Comparison of CPD for various tabs at NPR 3.*

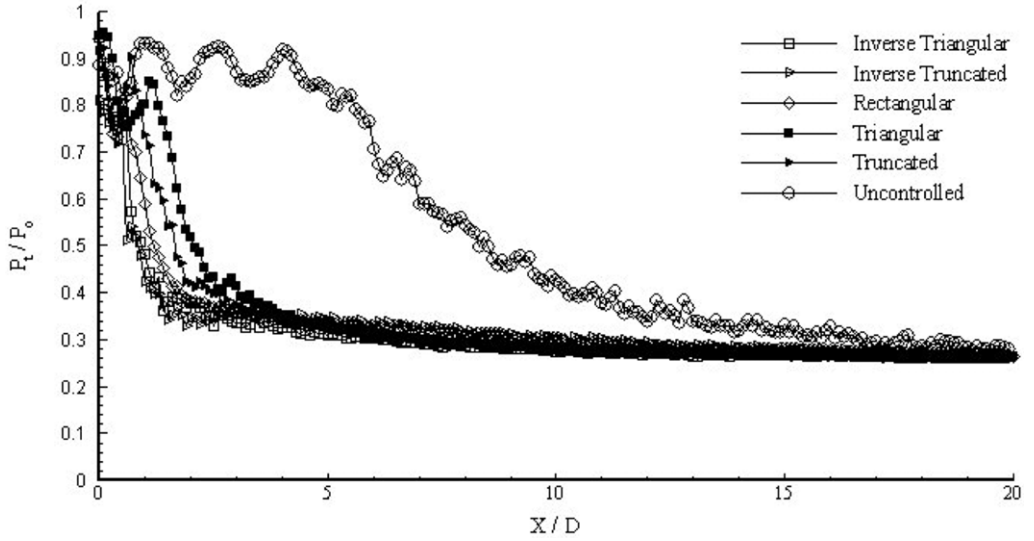


Figure 6. *Comparison of CPD for various tabs at NPR 4.*

pressure of the atmosphere to which the jet is discharged. The oblique shock from the opposite edges of the nozzle exit would cross each other at a distance downstream of the nozzle exit. For the present case of the axisymmetric nozzle, this shock crossover point would be at the jet axis, which is also the nozzle axis. After crossing over, the oblique shocks would get reflected from the barrel shock as expansion waves, since reflection from a free boundary is unlike (opposite) [1]. These expansion waves would travel up to the opposite boundary of the jet and get reflected as compression waves. Thus, there is a large number of compression and expansion waves prevailing in the near-field of the jet, where the flow Mach number is supersonic. It is essential to realise that, the flow Mach number downstream of the oblique shocks at the nozzle exit would be supersonic, but with its Mach number less than that upstream of the shock. This is because all the naturally occurring oblique shocks are weak. Thus, along the jet axis, the flow passes through several compression wave crossover points and expansion wave crossover points. This process will continue up to the end of the supersonic core. From Fig. 5, it is seen that the

https://doi.org/10.1017/aer.2025.10098 Published online by Cambridge University Press

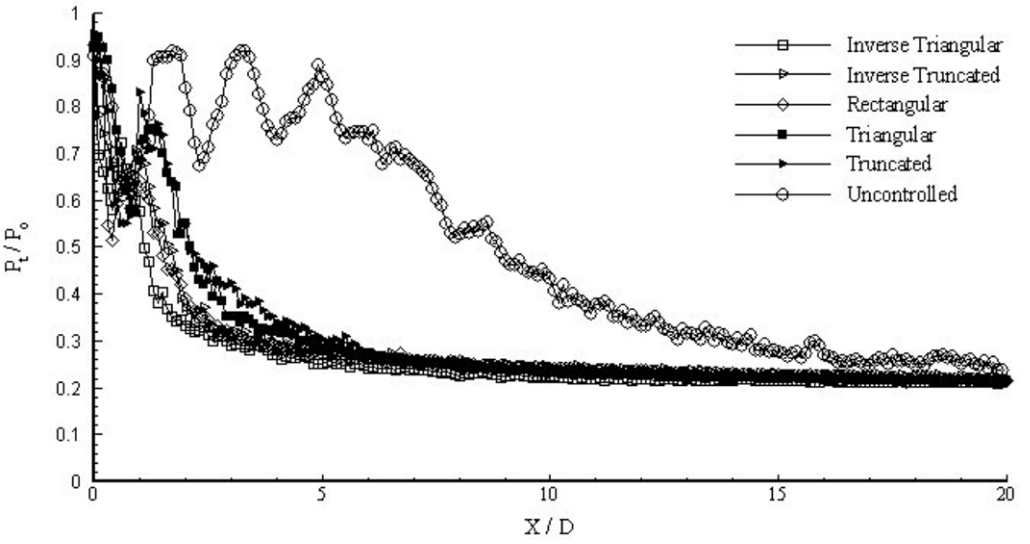


Figure 7. *Comparison of CPD for various tabs at NPR 5.*

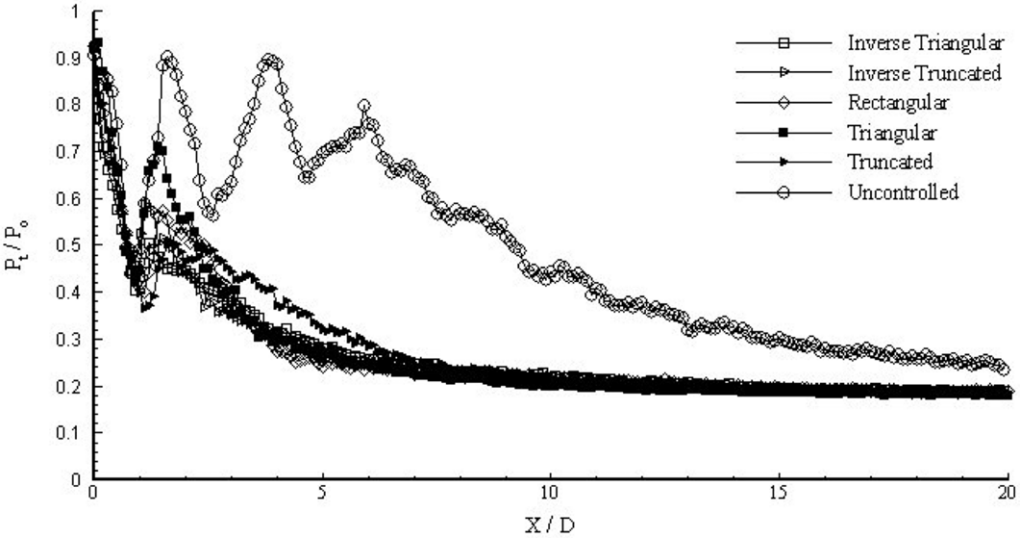


Figure 8. *Comparison of CPD for various tabs at NPR 6.*

decay of controlled jets is steeper than the uncontrolled jet, indicating that the mixing in the controlled jet is superior to the uncontrolled jet. The controlled jet is found to experience higher mixing in all three zones of the jet, namely the core, characteristic decay and fully developed zones. Among the tabs, the inverse truncated triangular tab causes faster decay than the others. The reason for the better mixing performance of the triangular tab (Fig. 4a and b) than the other two tabs (Fig. 4d and e) in accordance with the vortex dynamics, which states that the mixing promotion caused by a tab would be the best if the tab is capable for shedding mixing-promoting small-scale vortices of continuously varying size [1]. This is because the size of the vortex leaving the tab-edge is proportional to the tab's half-width at that location.

The tabs at the nozzle exit could able to promote the near-field mixing considerably, resulting in the reduction of the core length. Core length and its percentage reduction for different tabs tab, for NPR 3, are given in Table 1.

https://doi.org/10.1017/aer.2025.10098 Published online by Cambridge University Press

Table 1. *Core length for NPR 3*

Tabs	Triangular	Inverse triangle	Truncated triangle	Inverse truncated triangle	Rectangular
Core length (D)	0.9	0.4	0.6	0.3	0.5
% Reduction in core length	71	87	81	90	84

Table 2. *Core length for NPR 4*

Tabs	Triangular	Inverse triangle	Truncated triangle	Inverse truncated triangle	Rectangular
Core length (D)	1.1	0.5	0.7	0.5	0.6
% Reduction in core length	72	87	72	87	85

From the table, it is seen that all the tab configuration in the present study promotes the mixing considerably. The maximum mixing is for the inverse truncated triangular tab, which reduces the core length by about 90%, and the minimum is for the triangular tab, which amounts to only 70%. This shows that the mixing efficiency of the small-scale vortices shed from the tab is influenced by the shape of the tab. In accordance with vortex dynamics [1], it can be envisaged that the triangular tab with sharp and truncated vertex would shed mixing-promoting vortices and continuously varying size, which is congenial for mixing promotion, where this feature is missing in the case of the rest of the tabs. Another special feature is that vortices shed by the triangular tab will have the largest size of the small-scale vortex at the nozzle wall, whereas the inverse triangle will shed the smallest vortex closer to the nozzle axis. This difference will significantly influence the mixing-promoting capability of the triangular tab.

Mixing of controlled jets in the far field region (after $X/D = 15$) is more or less similar to that of the uncontrolled jet and the mixing is retarded by controlled jets at all three zones, namely the core, characteristic decay and fully developed zone. The controlled jets became fully developed at about $5D$ whereas the uncontrolled jet becomes fully developed only beyond 13D. Also, controlled jets possess weaker waves than uncontrolled jets, as seen from the amplitude of pressure variations. From Fig. 5, it is evident that the inverse truncated triangular tab is the most efficient among other tab configurations studied. However, the tabs at the nozzle exit result in severe penalties in terms of momentum and thrust loss since they block the nozzle exit area, in addition to the drag associated with it.

The percentage reduction in core length for a controlled jet is defined as,

$$\%\text{Reduction in core length} = \left[(\text{Core})_{\text{uncontrolled jet}} - (\text{Core})_{\text{controlled jet}}\right] / (\text{Core})_{\text{uncontrolled jet}} \times 100$$

The centreline decay of the controlled and uncontrolled jets at NPR 4 are compared in Fig. 6. NPR 4 is also an overexpanded state for the jet with a reduced level of adverse pressure gradient than NPR 3. The overexpansion level (P_e/P_a) for NPR 4 is 0.94. At this NPR also, the controlled jets are found to decay faster than the uncontrolled jets at alee all three zones. The tabs at the nozzle exit promoted considerable near-field mixing compared to far-field, resulting in the reduction of core length. The core length reduction caused by different tabs is given in Table 2. The core length of the uncontrolled jet extends up to $X/D = 4$. At this overexpanded state, different tab geometries are found to cause a significant core reduction, but the inverse triangular and inverse truncated triangular is the most efficient in the present study. The core length reduction caused by inverse triangular and inverse truncated triangular is 87% concerning uncontrolled jet. The truncated triangular and triangular tabs are found to cause a minimum core reduction of 72% at this NPR. The controlled jets became fully developed at about $X/D = 7$ whereas uncontrolled jets became fully developed after $X/D = 16$.

https://doi.org/10.1017/aer.2025.10098 Published online by Cambridge University Press

Table 3. *Core length for NPR 5*

Tabs	Triangular	Inverse triangle	Truncated triangle	Inverse truncated triangle	Rectangular
Core length (D)	1.3	0.6	1.4	0.9	1
% Reduction in core length	73	87.5	71	81	79

Figure 6 also reveals that the waves present in the core of controlled jets are weaker than the uncontrolled jets. Centreline pressure decay for this NPR initially shows a large decrease in pitot pressure followed by a rise which signifies the presence of Mach disk. After the Mach disk, the shocks in the orifice jet become weaker compared to the shocks in the nozzle jet.

The mixing promotion caused by the inverse triangular and inverse truncated triangular tabs is very prominent. From the above discussion, it can be concluded that for inverse triangular and inverse truncated triangular, mixing is better compared to other tabs and uncontrolled jets. For both cases of NPR 3 and NPR 4 in the present study, with a decrease in adverse pressure gradient, it is interesting to see the performance of different tabs.

The centreline decay of the jets at NPR 5 is compared in Fig. 7. NPR 5 is an underexpansion state for the jet. The underexpansion level (P_e/P_a) for NPR 5 is 1.17. The controlled jets continue to enjoy superior near-field mixing at this NPR. Also, they are found to decay faster than the uncontrolled jet at all three zones. Therefore, tabs at the nozzle exit promoted considerable near-field mixing compared to far-field, resulting in the reduction of core length. The core length reduction caused by different tabs is given in Table 3.

The core length of the uncontrolled jet extends up to $X/D = 4.9$. At this marginally underexpanded state, all the tab geometries are found to cause a substantial core reduction. As in NPR 4, the inverse triangular tab is the most efficient mixing promoter for NPR 5. The core length reduction caused by the inverse triangular tab is 87.5% concerning uncontrolled jet. The truncated triangular and triangular tabs are found to cause a minimum core reduction of 71% and 73% at this NPR. At this NPR, the location at which the controlled jets become fully developed moves downstream when compared to NPR 4. The controlled jets became fully developed at about $X/D = 8$ whereas uncontrolled jets became fully developed after $X/D = 18$. It is also seen that the waves present in the core of controlled jets are weaker than the uncontrolled jets.

The centreline decay results of controlled and uncontrolled jets at NPR 6, are compared in Fig. 8. NPR 6 is a case of a highly underexpanded state, with a favourable pressure gradient of 41% at the nozzle exit. The corresponding underexpansion level (P_e/P_a) for NPR 6 is 1.41. Like other NPRs, the controlled jets at NPR 6 are found to decay faster than the uncontrolled jet at all three zones, indicating superior mixing caused by all the tab configurations. The near-field decay is superior for all the tab configurations. As a result, the tabs at the nozzle exit caused considerable core length reduction compared to the uncontrolled jet. In addition, the tabs are found to weaken the waves significantly. It is interesting to see at NPR 6, that the centreline pressure curves of controlled jets initially show a large decrease in pitot pressure followed by a rise, which signifies the presence of Mach disk at around $X/D = 1$. After the Mach disk, the shocks in the orifice jet become weaker compared to the shocks in the nozzle jet. The core length reduction caused by different tabs is given in Table 4. The core length of the uncontrolled jet extends up to $X/D = 5.9$. The core length reduction caused by the inverse triangular tab is found to be maximum at NPR 6, which is about 79%. The truncated triangular and rectangular tabs cause a minimum core reduction of 56% and 62% at this NPR. The amplitude of pitot pressure oscillation of controlled jets is much less compared to uncontrolled jets which show the reduction in shock strength in the controlled jet. The controlled jets became fully developed at about $X/D = 10$ which has moved a little downstream as compared to NPR 5, whereas the uncontrolled jet became fully developed after $X/D = 18$.

https://doi.org/10.1017/aer.2025.10098 Published online by Cambridge University Press

Table 4. *Core length for NPR 6*

Tabs	Triangular	Inverse triangle	Truncated triangle	Inverse truncated triangle	Rectangular
Core length (D)	1.4	1.2	2.6	1.5	2.2
% Reduction in core length	76	79	56	74	62

3.2 Pressure profiles

The pitot pressure (P_t) distribution, measured along the tab (y-direction) and perpendicular to the tab (z-direction) of the controlled jets, is non-dimensionalised by dividing with the settling chamber pressure P_0. The distance in a direction along the tab (y-direction) and perpendicular to the tab (z- direction) is made non-dimensional by dividing them with nozzle exit diameter (D).

The pitot pressure distribution along the tab and perpendicular to the tab direction, at different axial locations especially in the near field up to $X/D = 10$ will be important in analysing whether the control forces the jet to become asymmetrical. To access this aspect, the pitot pressure profiles along the radial direction for the uncontrolled jet, and in the directions along and perpendicular to the tab for the controlled jet, at different axial locations ($X/D = 0.5$, 1, 2, 4, 6, 8 and 10) are presented in the Figs 9–19, for all the NPRs of the study.

The pressure profiles at $X/D = 0.5$, 2, 4, 6 and 10 for the uncontrolled jet operated at NPR 3 are shown in Fig. 9a. It is seen that in the near field from $X/D = 0.5$, 2 and 4 there are two high-pressure regions on either side of the jet axis. At $X/D = 6.0$ the profile exhibits a single peak, indicating that the jet has entered the characteristics decay zone. Also, at $X/D = 0.5$, there are two regions on either side of $Z/D = 0$. For $X/D = 2$ and 4, it has comparable pressure around $Z/D = 0$.

The pressure increases steeply to around 0.72 up to $Z/D = 0.5$ and then shows erratic behaviour up to $Z/D = 0.5$. To the left side of Z/D = 0.0, the value of P_t/P_0 is around 0.84, which is a minimum between $Z/D = 0.5$ to 0.5, implying that the velocity of the jet is maximum at the centre. At $X/D = 2.0$ also more or less the same trend is followed by the pressure profile as in the case of the pressure profile at $X/D = 0.5$. Both these locations are within the core region of the jet. At $X/D = 6.0$, which is in the characteristic decay region, the larger spread of the pressure profiles implies faster mixing. Finally, at $X/D = 10.0$, the jet has encountered the characteristic decay and the pitot pressure decay shows an almost fully developed nature.

In Fig. 9b–h the pressure profiles, along the tab and normal to the tab, are presented for the jet controlled with truncated triangular, rectangular, triangular and truncated triangular tabs, at NPR 3, are shown. For controlled jets, inverse triangular and inverse truncated triangular (having a core length of 0.4 and 0.3), the jet has entered into a characteristic decay zone for $X/D = 0.5$. For $X/D = 6$ and further, it can be inferred that the jet has entered into the fully developed zone. For triangular, truncated triangular and rectangular, $X/D = 0.5$ is in the core region. For the triangular tab, at $X/D = 0.5$ pressure starts rising from $Y/D = -0.4$ assuming the maximum value of 0.86 and then there is a dip and then pressure goes to its minimum value at $Y/D = 0$ which implies that the jet velocity is maximum at this point. For $X/D = 6$ and further, the jet is in the fully developed zone. For $X/D = 2$, it is in the characteristics decay zone. For the same tab, the spread perpendicular to the tab direction is more as compared to the spread along the tab direction. It is seen that, because of the intense interaction of vortices, there is some asymmetry introduced to the jet both along and perpendicular to the tabs as expected. However, asymmetry is not abnormal as seen in the figures above from Fig. 9b–h. For controlled jets, it is interesting to see that the spread normal to the tab has a larger magnitude as compared to the spread along the tab. This spread can be taken as an advantage from the jet mixing point of view. Pressure profiles shown in these figures (Fig. 9b–h) exhibit that the asymmetry introduced by the tabs in the direction along the tab is more compared to the direction perpendicular to the tab.

Pressure profiles for the uncontrolled jet at NPR 4 is shown in Fig. 10.

https://doi.org/10.1017/aer.2025.10098 Published online by Cambridge University Press

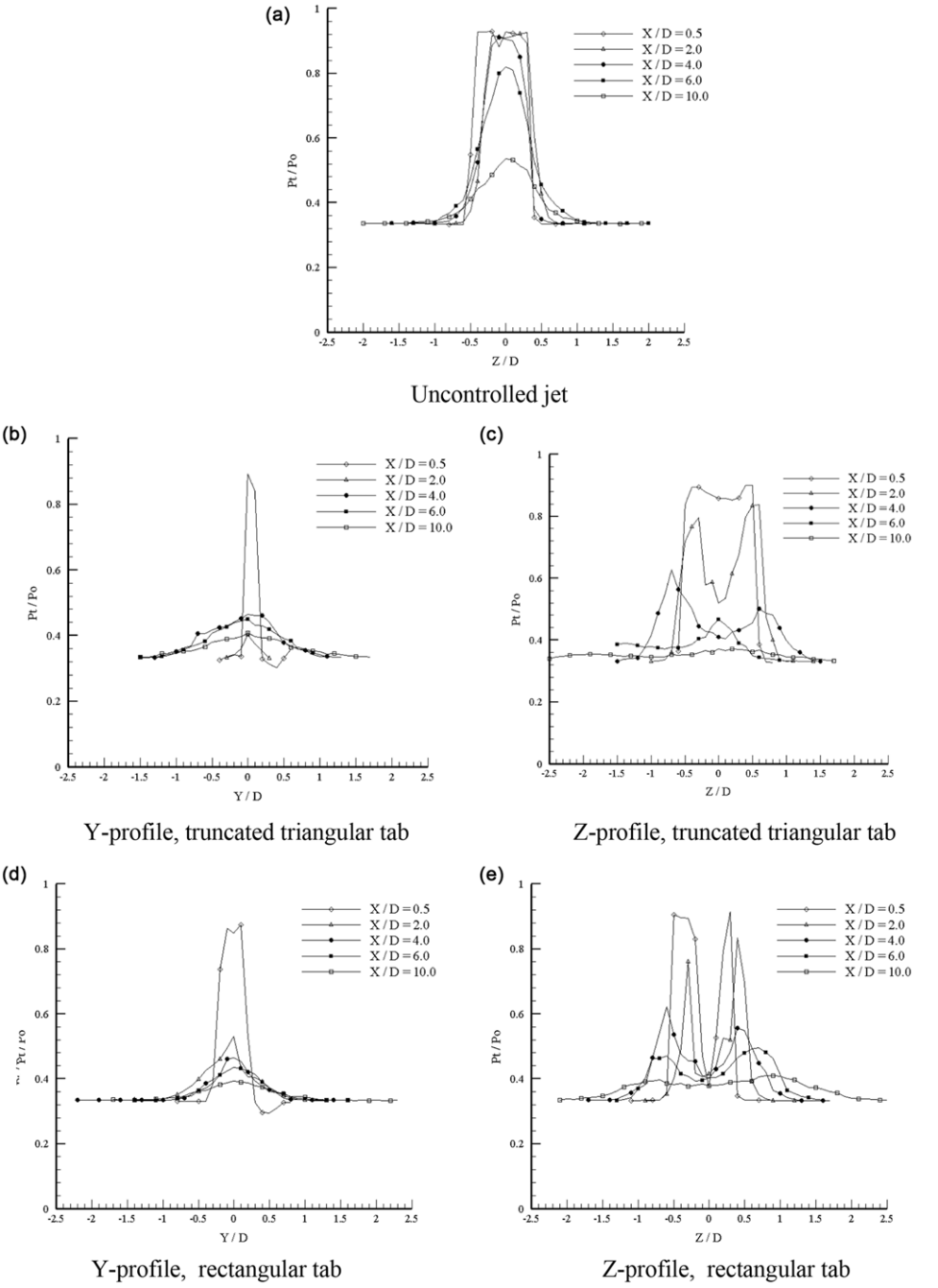
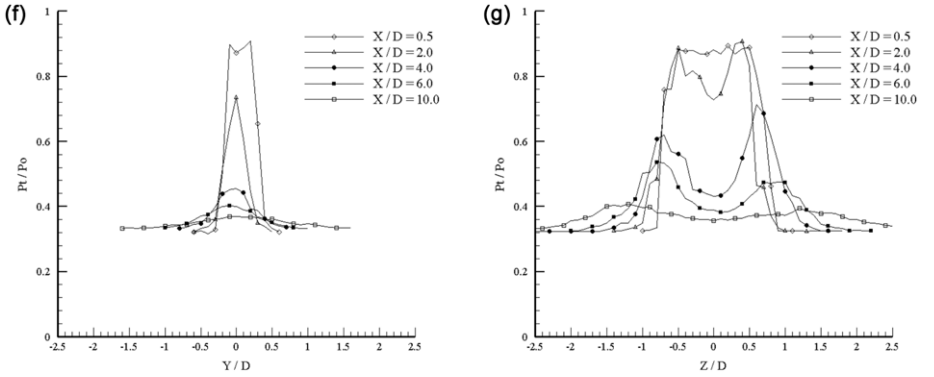


Figure 9. *Pressure profiles for NPR 3. (a) Uncontrolled jet (b) Y-profile, truncated triangular tab (c) Z-profile, truncated triangular tab (d) Y-profile, rectangular tab (e) Z-profile, rectangular tab (f) Y-profile, triangular tab (g) Z-profile, triangular tab.*

https://doi.org/10.1017/aer.2025.10098 Published online by Cambridge University Press



Y-profile, triangular tab Z-profile, triangular tab

Figure 9. *Continued.*

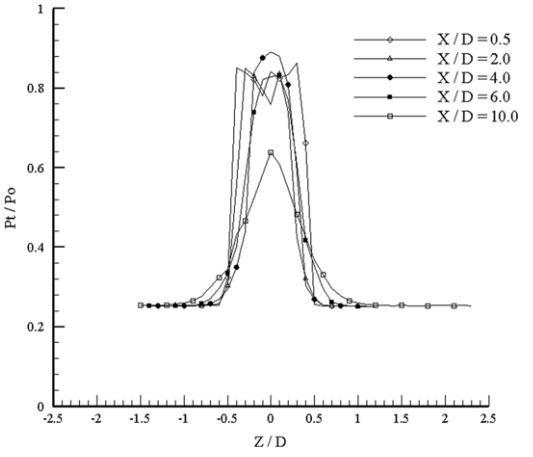


Figure 10. *Pressure profiles for uncontrolled jet at NPR 4.*

For NPR 4, which is also in the overexpansion region, for uncontrolled jet, up to $X/D = 4$, the jet is in the core region, $X/D = 6$ it is in the characteristics decay zone and for $X/D = 10$ it is in the fully developed zone (Fig. 10). Here it is interesting to note that the spread is not symmetric for different tabs along the tab and perpendicular to the tab directions. The overexpansion level has decreased. In a fully developed zone, at $X/D = 10$, for an uncontrolled jet, the pressure level is at 0.6, but for a controlled jet, it is below 0.4, which indicates that mixing is very prominent in the controlled jet. There is some asymmetry in both directions. This asymmetry introduced by the vortices shed by tabs is sensitive to the expansion level at the nozzle exit. For tabs at $X/D = 8$ and $X/D = 10$, the jet is in a fully developed region. It can also be observed that the decay is different in both directions for all tabs. For rectangular, truncated triangular, inverse triangular and inverse truncated triangular, the jet is in the characteristic decay zone even for $X/D = 1$, but for triangular tab, it is in the core region.

For the uncontrolled jet, at NPR 5, which is an underexpanded jet, up to $X/D = 4$, the jet is in the core region. At $X/D = 6$ and 10, it is in the characteristic decay zone as evident from Fig. 11a. For inverse triangular (Fig. 11b) and inverse truncated triangular (Fig. 11c), $X/D = 0.5$ is in the core region, $X/D = 2$, 4 and 6 are in the characteristics decay zone and $X/D = 10$ is in the fully developed zone. The pressure plots for the jet controlled with inverse triangular tab that resulted in the best jet mixing, leading to 87.5% core length reduction of this study, shown in Fig. 11b and c, compliment the centreline decay in Fig. 7. But for triangular, truncated triangular and rectangular up to $X/D = 1$ it is in the core region, for

https://doi.org/10.1017/aer.2025.10098 Published online by Cambridge University Press

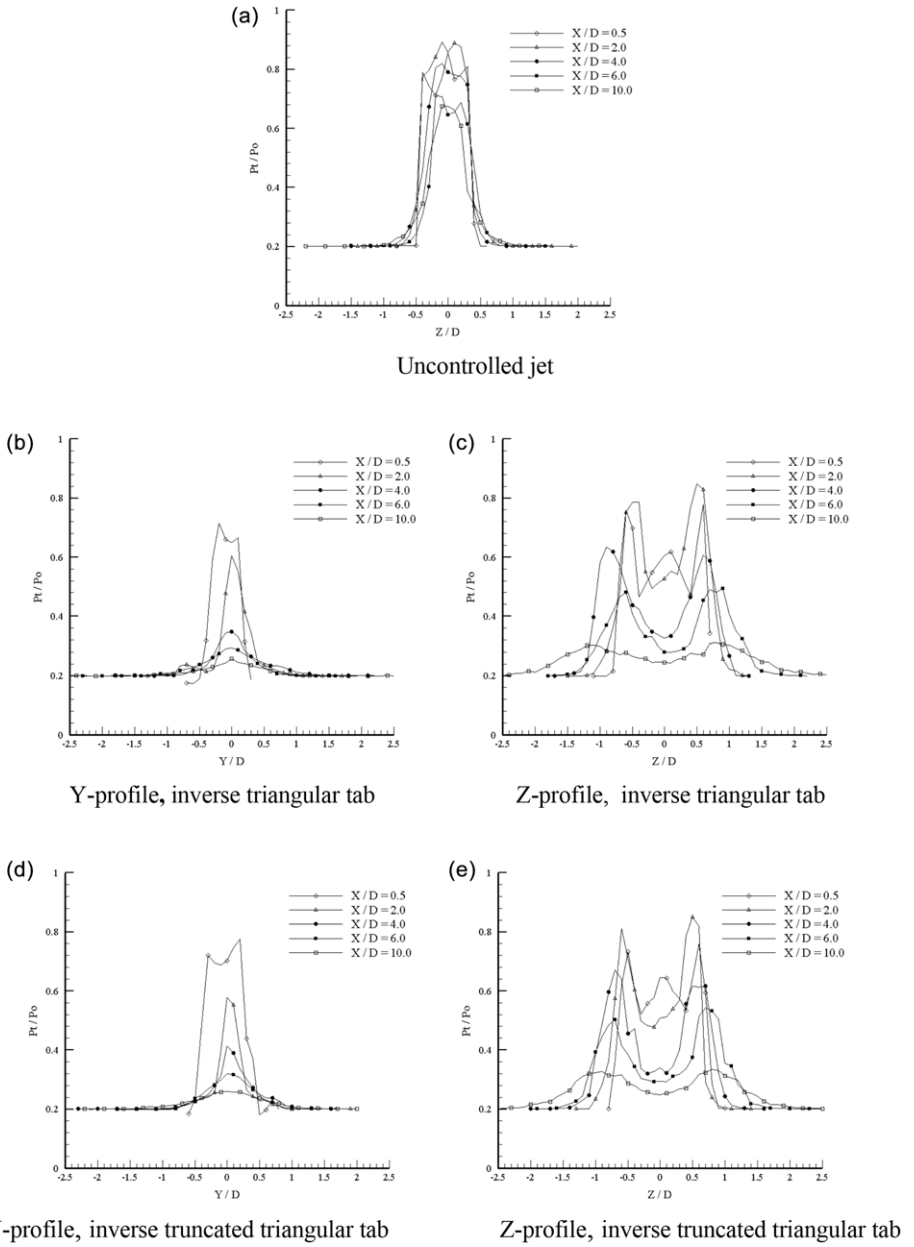


Figure 11. *Pressure profiles for NPR 5 11(a) Uncontrolled jet (b) Y-profile, inverse triangular tab (c) Z-profile, inverse triangular tab (d) Y-profile, inverse truncated triangular tab 11(e) Z-profile, inverse truncated triangular tab.*

X/D = 2, 4 and 6 it is in the characteristic decay zone and for *X/D* = 10, the jet is in the fully developed zone. For all tabs, the spread direction perpendicular to the tab is more as compared to the spread in the direction along the tab. The pressure level for all the tabs at *X/D* = 10 are comparable. Pressure levels for all the tabs at this NPR at all locations are lower as compared to uncontrolled jets. Decay for tabs along and perpendicular to the tab directions are different. There is asymmetry for the tabs, which is due to the vortices shed by the tabs to the expansion level at the nozzle exit.

https://doi.org/10.1017/aer.2025.10098 Published online by Cambridge University Press

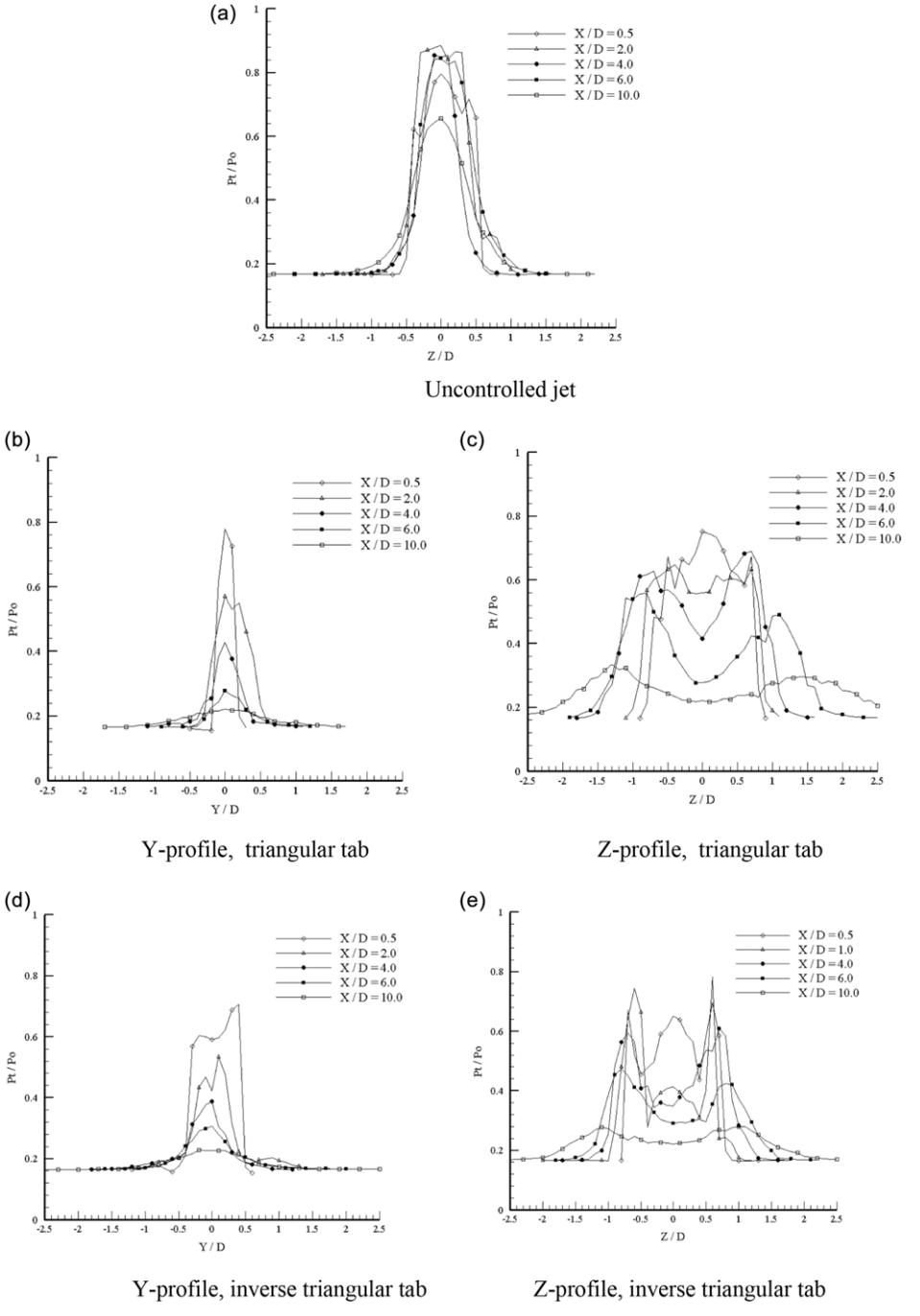


Figure 12. *Pressure profiles for NPR 6 (a) Uncontrolled jet (b) Y-profile, triangular tab (c) Z-profile, triangular (d) Y-profile, inverse triangular tab (e) Z-profile, inverse triangular tab (f) Y-profile, truncated triangular tab (g) Z-profile, truncated triangular tab (h) Y-profile, rectangular tab (i) Z-profile, rectangular tab.*

https://doi.org/10.1017/aer.2025.10098 Published online by Cambridge University Press

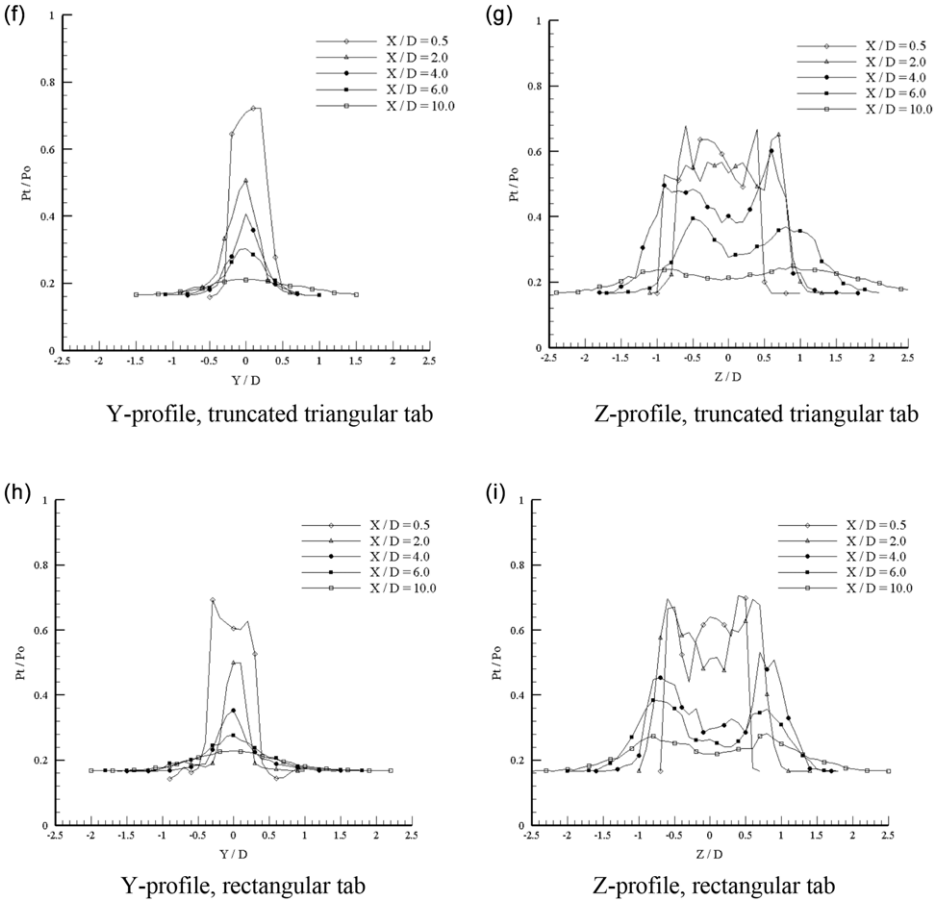


Figure 12. *Continued.*

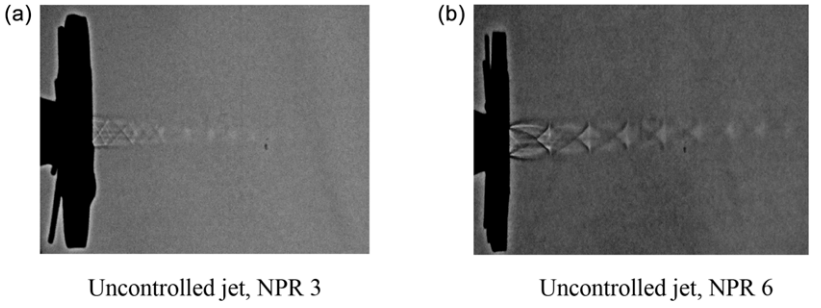


Figure 13. *(a) Uncontrolled jet, NPR 3 (b) uncontrolled jet, NPR 6.*

Pressure profiles for the jet at NPR 6 are shown in Fig. 12a–i. For the uncontrolled jet, at NPR 6, with a level of underexpansion of 1.41, up to $X/D = 4$, the jet is in the core region. It is seen that in the profile plot along the tab at $X/D = 0.5$, it does not exhibit any dip. At $X/D = 6$ and 10, it is in the characteristic decay zone as evident from Fig. 11a. For inverse triangular, triangular and inverse truncated triangular, $X/D = 0.5$ and 1 is in core regions 2, 4 and 6 are in the characteristics decay zone and for $10D$ it is in the fully developed zone. But for truncated triangular and rectangular up to $X/D = 2$ it is in the core region, for $X/D = 4$ and 6 it is in the characteristic decay zone and for $X/D = 10$, the jet is in the fully developed zone. The jet was rendered more asymmetrical compared with the uncontrolled jet. For all tabs, the

https://doi.org/10.1017/aer.2025.10098 Published online by Cambridge University Press

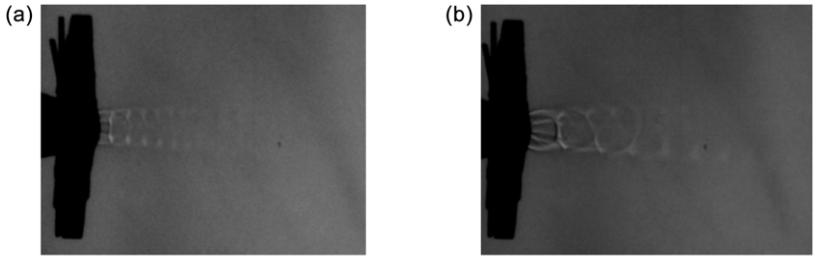


Figure 14. *(a) Inverse triangle (b) inverse triangle (along the tab), NPR 3 (along the tab), NPR 6.*

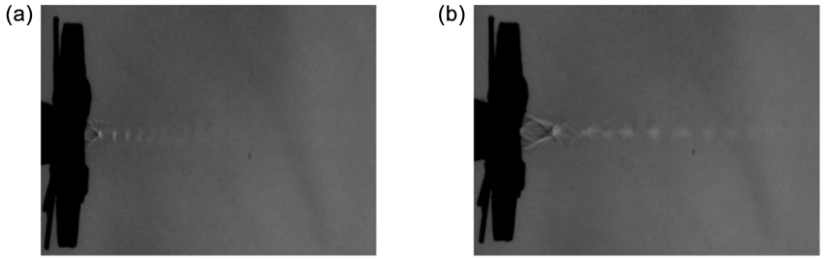


Figure 15. *(a) Inverse triangle (b) inverse triangle (normal to the tab), NPR 3 (normal to the tab), NPR 6.*

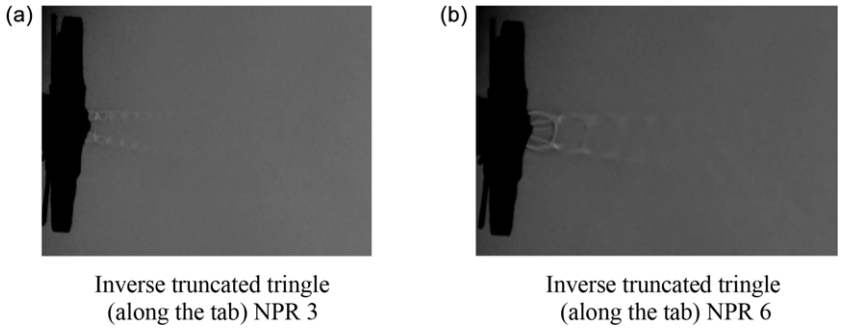


Figure 16. *(a) Inverse truncated tringle (b) inverse truncated tringle (along the tab) NPR 3 (along the tab) NPR 6.*

spread perpendicular to the tab direction is more as compared to the spread along the tab direction. The pressure level (P_t/P_0) for all the tabs at $X/D = 10$ are comparable. Pressure levels for all the tabs at all the locations are lower compared to uncontrolled jets. Decay along the tab and perpendicular to the tab directions are different. There is asymmetry for the tabs, which is due to the vortices shed by the tabs at the nozzle exit.

3.3 Shadowgraph

The shadowgraph technique was used to visualise the waves prevalent in the jets, with and without control, at different NPRs of the present study. For controlled jets, visualisation has been carried out viewing along and normal to the tabs. Shadowgraph pictures of a circular jet of Mach number 1.6, with

https://doi.org/10.1017/aer.2025.10098 Published online by Cambridge University Press

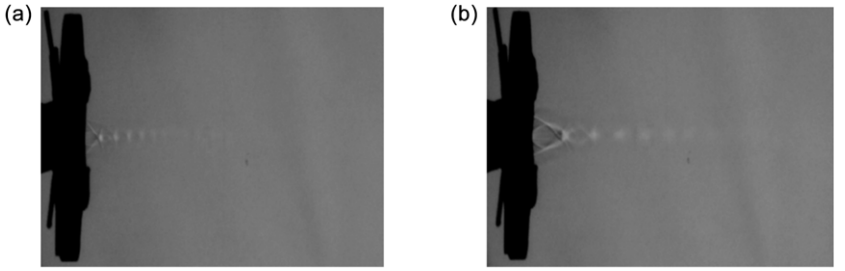


Figure 17. *(a) Rectangular tab (b) rectangular tab, (perpendicular to the tab) NPR 3 (perpendicular to the tab) NPR 6.*

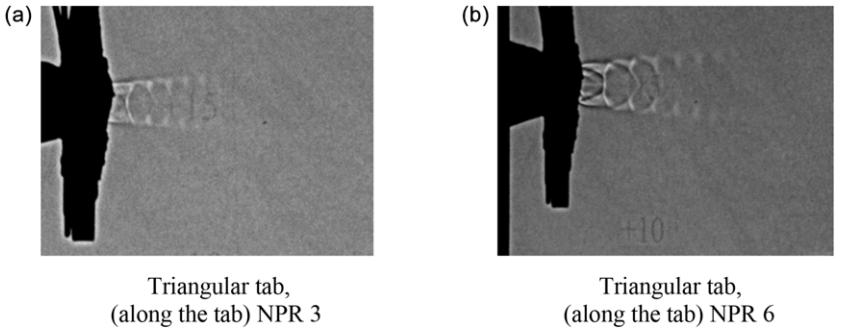


Figure 18. *(a) Triangular tab, (b) triangular tab, (along the tab) NPR 3 (along the tab) NPR 6.*

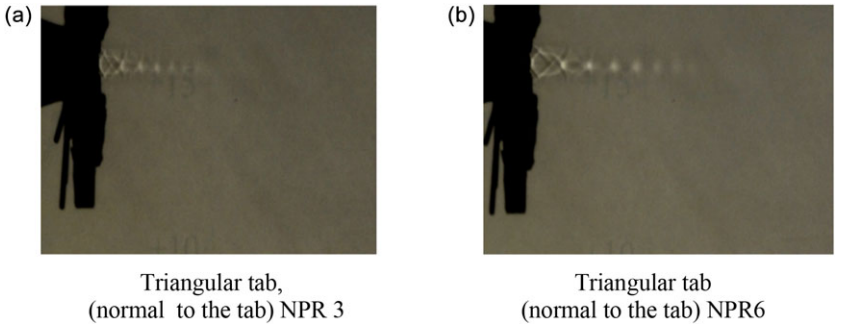


Figure 19. *(a) Triangular tab, (b) triangular tab (normal to the tab) NPR 3 (normal to the tab) NPR6.*

inverse triangular, inverse truncated triangular, rectangular, triangular and truncated triangular tabs at NPRs 3 to 6 are shown in Figs 13 to 21. The shadowgraphs of the uncontrolled jet for NPRs 3 to 6 are shown in Fig. 13a–13b.

The shadowgraph of the uncontrolled circular jet at NPR 4 shows that oblique shocks are formed at the nozzle exit. In an overexpanded jet, there would be an oblique shock due to overexpansion and an expansion fan due to the relaxation prevailing at the nozzle exit. The oblique shock cone at the nozzle exit terminates as a shock cross-over at the jet axis and reaches the barrel shock. On reaching the barrel shock, the oblique shock reflects as an expansion fan, since reflection from the fluid boundary is unlike. The kinks formed at the shock reflection points are seen in the picture. The expansion waves cross each other reach the boundary and reflect as compression waves. The reflected compression waves once again cross each other at the jet axis and reflect as an expansion fan from the barrel shock boundary.

https://doi.org/10.1017/aer.2025.10098 Published online by Cambridge University Press

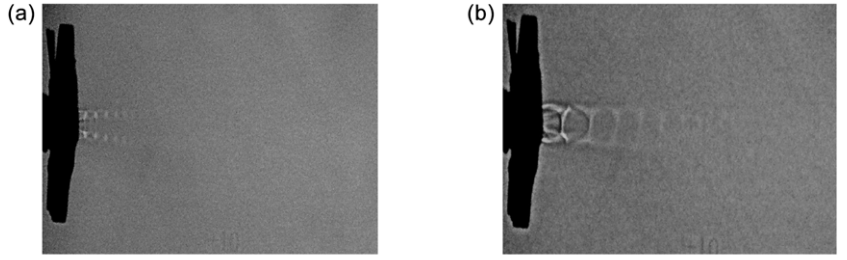


Figure 20. *(a) Truncated triangular tab, (b) truncated triangular, (along the tab) NPR 3 (along the tab) NPR 6.*

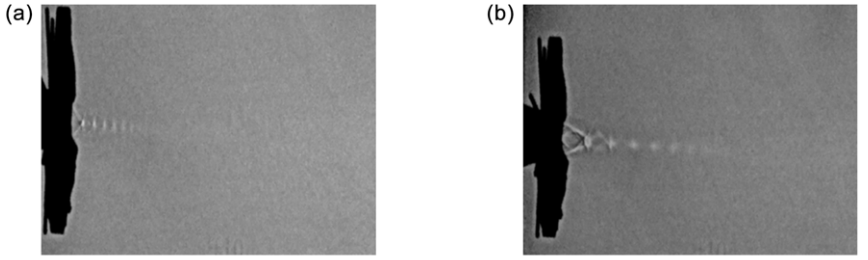


Figure 21. *(a) Truncated triangular tab, (b) truncated triangular tab, (normal to the tab) NPR 3 (normal to the tab) NPR6.*

This kind of wave reflection continues to some downstream distance. The distance between successive shock reflection points is called a shock cell.

In Fig. 20a two cells can be seen clearly and the rest are feeble. These oblique shocks cross each other at the jet axis and reach the barrel shock. The distance between successive shock reflection points (kinks) is called shock cell length. NPR 4 is also overexpanded but with an adverse pressure gradient less than that of NPR 3. Therefore oblique shock at the nozzle exit is weaker, which led to the cross-over point slightly downstream. At NPR 5 the jet is underexpanded, so it encounters an expansion fan due to the relaxation effect. This expansion gets reflected as compression waves and the process continues. Here, two prominent cells can be seen and others are feeble. In Fig. 13b, at NPR 6 same process continues with more cells visible. From the visualisation pictures of the controlled jets with different tabs it is seen that the core region is less wave-dominated as compared to the uncontrolled jet. The shadowgraph pictures demonstrate the difference in wave domination in the supersonic core and the effect of mixing augmentation due to the tabs of the present study. It is well known that shock cell length reduction and weakening of waves in the jet core can be taken as a measure of reduced shock-associated noise [26]. Therefore, it can be justifiably stated that even though jet noise has not been measured, the control with tabs is advantageous from a jet noise reduction point of view. In all the above cases shock cells can be observed to progressively reduce in size with an increase in axial distance from the nozzle exit. Controlled configurations with tabs of different geometries in the present work, display reduced shock cell widths when viewed along the z-axis than when viewed along y-axis. Shadowgraph results complement the findings of centreline pressure decay, namely the core length, shock cell length and the presence of Mach disc at highly underexpanded NPR 6.

https://doi.org/10.1017/aer.2025.10098 Published online by Cambridge University Press

4.0 Conclusions

The results of this investigation clearly show that the mixing-promoting effectiveness of the inverse triangular and inverse truncated triangular tab is superior to rectangular, upright triangular and upright truncated triangular tabs. Core length reduction of 87% is achieved with inverse triangular tabs at NPR 3, 4 and 5. The corresponding core length reductions caused by the upright triangular upright truncated triangular, and rectangular tabs are about 71, 81 and 84%, respectively. The jet spreads in the direction perpendicular to the tab more than in the direction along the tab. The pressure profiles also support the inference made from the centreline pressure decay that the tabs enhance jet mixing and are superior to the uncontrolled jet. The shadowgraph pictures for the uncontrolled and controlled jets demonstrate the effectiveness of tabs in weakening the waves in the jet core. Among the tabs, the inverse truncated triangular tab causes faster decay than the others.

Acknowledgement. My sincere thanks to my Master's student, Chandan Satyarth, for conducting the experiments of this study.

References

[1] Rathakrishnan, E. *Applied Gas Dynamics*, 2nd ed, John Wiley, 2019, West Sussex, UK.
[2] Miller, R.S., Madina, C.K. and Givi, P. Numerical simulation of non-circular jets, *Comput. Fluids*, 1995, **24** (1), pp 1–25.
[3] Quinn, W.R. Experimental study of the near field and transition region of a free jet issuing from a sharp-edged elliptic orifice plate, *Eur. J. Mech*, 2007, **26**, pp 583–614.
[4] Grinstein, F.F., Gutmark, E. and Parr, T. Near field dynamics of subsonic free square jets. A computational and experimental study, *Phys. Fluids*, 1995, **7** (6), pp 1483–1497.
[5] Gutmark, E., Schadow, K.C. and Wilson, K.J. Subsonic and supersonic combustion using noncircular injectors, *J. Propulsion*, 1991, **7**, (2), pp 240–249.
[6] Clement, S., Murugan, K.N. and Rathakrishnan, E. Superiority of elliptical jets, *IE(I) Journal-AS*, 2005, **86**, pp 1–7.
[7] Bradbury L.J.S and Khadem A.H. The distortion of a jet by tabs, *J. Fluid Mech.*, 1975, **70**, pp 801–813.
[8] Ahuja, K.K. and Brown. W.H. Shear flow control by mechanical tabs, AIAA Paper 89-0994, 1989.
[9] Ahuja, K.K. Mixing enhancement and jet noise reduction through tabs plus ejectors, AIAA Paper 93-4347, 1993.
[10] Brown, G.L. and Roshko, A. On destiny effects and large structure in turbulent mixing layers, *J. Fluid Mech.*, 1974, **64** (4), pp 775–816.
[11] Reeder, M.F. and Samimy, M. The evolution of a jet with vortex-generating tabs: real-time visualization and quantitative measurements, *J. Fluid Mech.*, 1996, **311**, pp 73–118.
[12] Zaman, K.B.M.Q, Reeder, M.F. and Samimy. M. Control of an Axisymmetric jet using vortex generators, *Phys. Fluids*, 1994, **6**, pp 778–793
[13] Steffen, C.J., Reddy, D.R. and Zaman, K.B.M.Q. Numerical modelling of jet entrainment for nozzles fitted with delta tabs, AIAA Paper 97-0709, 1997.
[14] Zaman, K.B.M.Q. Streamwise vorticity generation and mixing enhancement in free jet by delta-tabs, AIAA Paper 93-3253, 1993.
[15] Carletti, M.J., Rogers, C.B. and Parekh, D.E. Use of streamwise vorticity to increase mass entrainment in a cylindrical ejector, *AIAA Journal*, 1995, **33**, pp 1641–1645.
[16] Bohl. D, and Foss, J.F. Enhancement of passive mixing tabs by the addition of secondary tabs, AIAA Paper 96-054, 1996.
[17] Grosch, C.E, Seiner, J.M, Hussaini, M.Y, and Jackson, T.L. Numerical simulation of mixing enhancement in a hot supersonic jet, *Phys. Fluids*, 1997, **9**, pp 1125–1143.
[18] Feng, T, and McGuirk, J.J. LDA measurements of underexpanded jet flow from an axisymmetric nozzle with tabs, 3rd AIAA Flow Control Conf., AIAA–2006-3702, 2006.
[19] Behrouzi, J. and McGuirk, P. Experimental studies of tab geometry effects on mixing enhancement of an Axisymmetric jet, *JSME Int. J., Series B*, 1998, **41** (4), pp 908–917.
[20] Thanigaiarasu, S, Jayaprakash, S, Elangovan, S and Rathakrishnan, E "Influence of tab geometry and its orientation on underexpanded sonic jets", institute of mechanical engineers (UK), part G, *J Aerosp Eng*, 2008, **222**, pp 331–339.
[21] Lovaraju, P, Paparao, K.P.V. and Rathakrishnan, E. Shifted cross-wire for supersonic jet control, AIAA Paper 2004-4080, 2004.
[22] Chiranjeevi Phanindra, B. and Rathakrishnan, E. Corrugated tabs for supersonic jet control, *AIAA Journal*, 2010, **48** (2), pp 453–465.
[23] Arun Kumar, P and Rathakrishnan, E. Triangular tabs for supersonic jet mixing enhancement, *Aero J. -New Series*, 2014, **118** (1209), pp 1245 –1278. doi: 10.1017/S0001924000009969
[24] Arun Kumar, P and Rathakrishnan, E. Truncated triangular tabs for supersonic-jet control, *J. Prop. Power*, 2013, **29** (1), pp 50–65. doi: 10.2514/1.B34642

https://doi.org/10.1017/aer.2025.10098 Published online by Cambridge University Press

[25] Rathakrishnan, E Effect of tab length on supersonic jet mixing, *Phys. Fluids*, 2022, **34**, pp 096109. doi: 10.1063/5.0113192
[26] Rathakrishnan, E. Effect of corrugation on limiting arc-tab mixing performance, *Phys. Fluids*, 2022, **34**, pp 116124. doi: 10.1063/5.0127031
[27] Rathakrishnan, E. *Instrumentation, Measurements and Experiments in Fluids*, CRC Press, 2009, Boca Raton, New York.

Cite this article: Rathakrishnan E. (2026). Tab orientation effect on jet mixing. *The Aeronautical Journal*, **130**, 657–679. https://doi.org/10.1017/aer.2025.10098

https://doi.org/10.1017/aer.2025.10098 Published online by Cambridge University Press